

## RESEARCH ARTICLE

## Genomic insights into chromium resistance mechanisms in *Citrobacter* spp.

Lianbin Cao, Zixin Dou, Luxin Wang, Ye Tao, Tong Li, Wentong Li, Guangchuan Shi, Enzhong Li, Hongmei Sun\*

School of Biological Science and Food Engineering, Huanghuai University, Zhumadian, Henan, China.

Received: May 18, 2025; accepted: August 29, 2025.

Cr(VI) is a highly toxic environmental pollutant, and microbial reduction represents a promising bioremediation strategy. This study investigated the Cr(VI)-reducing capability of *Citrobacter freundii* A1B10 and elucidated its genomic determinants. When *C. freundii* A1B10 was inoculated in LB medium containing 8.5 mg/L Cr(VI), the residual Cr(VI) was  $3.48 \pm 1.31$  mg/L after 40 h incubation. Whole-genome sequencing of *C. freundii* A1B10 showed 4,927,083 bp with 4,631 coding genes and a GC content of 52.11%. Genomic analysis identified critical determinants for Cr(VI) resistance including sulfate (*ettA*, *cysA*, *cysW*, *cysU*, *cysP*), phosphate (*pstS*, *pstC*, *pstA*, *pstB*, *phoU*), and molybdate (*modF*, *modC*, *modE*, *modB*, *modA*) transporters, which implicated that  $\text{CrO}_4^{2-}$  was taken *via* competitive ion transport. Reduction pathways involved chromate reductase (*chrR*), cytochrome c (*ccmH*, *ccmF*, *ccmE*, *ccmG*, *nrfE*, *napC*, *napB*, *nrfB*, *torC*, *torA*, *torY*, *torZ*, *fbhH*, *petA*), nitrite reductases (*nirD*, *nirB*, *nrfA*), proton transport proteins (*atpB*, *atpE*, *atpF*, *atpH*, *atpA*, *atpG*, *atpD*, *atpC*), and cytochrome oxidases (*appX*, *cydB*, *cydA*, *cydX*, *cyoD*, *cyoB*, *cyoA*, *cyoC*). These systems collectively facilitated extracellular proton/electron transfer and intracellular Cr(VI)-to-Cr(III) reduction, thereby mitigating chromium toxicity. This study provided a genomic blueprint for *C. freundii* A1B10 of Cr(VI) resistance, highlighting multi-channel transport and enzymatic reduction mechanisms.

**Keywords:** Cr(VI); *Citrobacter freundii*; whole-genome sequencing; reduction.

\*Corresponding author: Hongmei Sun, School of Biological and Food Engineering, Huanghuai University, No. 76 Kaiyuan Road, Zhumadian, Henan 463000, China. Email: [sunhm58@163.com](mailto:sunhm58@163.com).

### Introduction

Chromium (Cr), a critical industrial metal, is extensively utilized in electroplating, tanning, metallurgy, and pigment manufacturing, resulting in annual emissions of 250 pounds into the atmosphere and 64,500 pounds into aquatic systems [1]. Among its compounds, hexavalent chromium (Cr(VI)) has emerged as a significant environmental and health hazard due to its strong oxidizability, high mobility, and bioaccumulation potential [2]. Cr(VI) enters

ecosystems *via* industrial wastewater, exhaust gases, and solid waste, persisting in soil and aquatic environments [3]. Toxicological studies revealed that Cr(VI) toxicity originated from its ability to penetrate cell membranes, where it generated reactive oxygen species (ROS), triggering DNA strand breaks, protein oxidation, and lipid peroxidation, ultimately resulting in apoptosis or carcinogenesis [4, 5]. To address chromium contamination, conventional physicochemical remediation technologies including chemical reduction, adsorption

precipitation, and ion exchange have been widely employed [6]. Chemical reduction methods utilize reducing agents such as  $\text{Fe}^{2+}$  and sodium thiosulfate ( $\text{Na}_2\text{S}_2\text{O}_5$ ) to convert Cr(VI) into less toxic Cr(III) [7, 8]. However, excessive reductants may induce secondary pollution [9]. Adsorption techniques, while effective for Cr(VI) removal from aqueous systems, face challenges such as high regeneration costs of common adsorbents like activated carbon and nanoscale zero-valent iron and the risk of heavy metal re-release during spent adsorbent disposal [10]. These limitations have driven researchers to explore more sustainable microbial remediation strategies.

The cornerstone of microbial remediation technology lies in leveraging the metabolic capabilities of specific bacterial strains to achieve efficient detoxification of Cr(VI) [11]. Research on microbial chromium resistance mechanisms serves as the core driver for advancing microbial remediation strategies for heavy metal pollution [12]. Currently identified microbial chromium resistance mechanisms include biosorption, biological reduction, and biomineralization [13-15]. For example, *Aspergillus niger* immobilizes Cr(VI) by forming stable complexes via polysaccharides and proteins on hyphal surfaces [16]. *Shewanella oneidensis* MR-1 reduces Cr(VI) to Cr(III) through a cytochrome c mediated extracellular electron transport chain [17]. *Pseudomonas putida* catalyzes the stepwise reduction of Cr(VI) via the NADPH-dependent ChrR enzyme with its antioxidant system mitigating oxidative stress during the process [18]. Under heavy metal stress, *Ochrobactrum tritici* 5bvl1 synthesizes polyphosphate to bind Cr(III), forming insoluble extracellular phosphate complexes that enhance community resistance [19]. By elucidating chromium resistance mechanisms in metal-tolerant microorganisms, researchers can optimize strain screening, genetic engineering, and remediation process design [20]. The revelation of these microbial chromium resistance mechanisms significantly enhance the efficiency, stability, and applicability of microbial remediation technologies, driving their development for practical environmental

applications [21]. In recent years, *Citrobacter* spp. has garnered significant attention in heavy metal pollution remediation due to its exceptional hexavalent chromium (Cr(VI)) reduction efficiency and remarkable environmental adaptability [22]. However, current research predominantly focuses on phenotypic characterization, while systematic elucidation of the molecular mechanisms underlying Cr(VI) reduction and the regulatory networks of resistance genes remain scarce. This knowledge gap critically hinders its application in engineered remediation systems.

This study employed whole-genome analysis to elucidate Cr(VI) uptake, efflux, and intracellular-extracellular reduction mechanisms in the chromium-resistant *C. freundii* A1B10. The results of this study provided a theoretical reference for systematically elucidating the chromium resistance mechanisms of chromium-resistant microorganisms. Meanwhile, this study also provided possible molecular targets for molecular biology approaches to optimize the chromium-resistant performance of *Citrobacter* spp.

## Materials and methods

### Strain and growth medium

*Citrobacter freundii* A1B10 was purchased from China General Microbiological Culture Collection Center (CGMCC, Beijing, China) with the CGMCC Number of 1.12836. Luria-Bertani (LB) medium was used as the basal growth medium comprising 10 g tryptone, 5 g yeast extract, and 10 g NaCl in one liter volume. All reagents were sourced from Sinopharm Chemical Reagent Co. (Shanghai, China). LB media were adjusted to pH 7.2 prior to autoclaving, and the bacteria were incubated at  $30 \pm 1^\circ\text{C}$ .

### Determination of Cr(VI) reduction efficiency

*C. freundii* A1B10 was cultured in Cr(VI)-supplemented LB medium at  $30 \pm 1^\circ\text{C}$  under shaking conditions of 180 rpm for 96 h. Uninoculated medium served as the abiotic

control. Residual Cr(VI) concentrations were quantified using the diphenylcarbazide spectrophotometric method [23]. An appropriate amount of colorless sample was taken, diluted to the mark in a 50 mL colorimetric tube, followed by addition of 0.5 mL sulfuric acid solution and 0.5 mL phosphoric acid solution, then 2 mL diphenylcarbazide chromogenic reagent. Absorbance was measured at 540 nm using a Thermo Scientific Multiskan SkyHigh Spectrophotometer (Thermo Fisher Scientific, Waltham, Massachusetts, USA). A calibration curve ( $R^2 = 0.9999$ ) was generated using Cr(VI) standards (0 – 20 µg/mL).

### Genomic DNA extraction

*C. freundii* A1B10 was cultivated in LB medium at  $30 \pm 1^\circ\text{C}$ , 180 rpm, for 24 h. The bacterial cells were harvested by centrifugation at 1,500 g for 10 min at  $4^\circ\text{C}$  with subsequent removal of supernatant. Bacterial DNA was purified using the Quick-DNA Miniprep Plus Kit (Zymo Research, Tustin, California, USA) with purity and integrity being assessed by agarose gel electrophoresis and quantified *via* Qubit 4.0 Fluorometer (Thermo Fisher Scientific, Waltham, Massachusetts, USA).

### Library construction and sequencing

Libraries for single-molecule real-time (SMRT) sequencing were constructed with an insert size of 10 kb using the SMRTbell® Template Prep Kit (version 1.0) (PacBio, Menlo Park, California, USA). Sequencing libraries were generated using NEBNext® Ultr™ DNA Library Prep Kit for Illumina (NEB, Omaha, Nebraska, USA) following manufacturer's instructions. The genome of *C. freundii* A1B10 was sequenced by Novogene (Sacramento, CA, USA).

### Whole genome map

GeneMarkS (version 4.17) (<http://topaz.gatech.edu/GeneMark/>) was used to predict the coding genes of the sequenced genome, while Clusters of Orthologous Groups (COG) (<http://www.ncbi.nlm.nih.gov/COG/>) was employed to predict gene functions. The assembled genomic sequences derived from

sequenced samples were integrated with coding gene prediction results and visualized using Circos software (version 0.69) (<https://circos.ca/>), ultimately generating a comprehensive whole genome map.

## Results

### Cr(VI) reducing capacity of *C. freundii* A1B10

The results demonstrated that, after 40 h incubation of LB media containing 8.5 mg/L Cr(VI) with/without inoculated *C. freundii* A1B10, the residual Cr(VI) concentration was reduced from 8.5 mg/L to  $3.48 \pm 1.31$  mg/L in the LB media with *C. freundii* A1B10, while the residual Cr(VI) concentration remained basically unchanged in the LB media without *C. freundii* A1B10 (Figure 1). The results confirmed that *C. freundii* A1B10 had the ability to reduce Cr(VI).

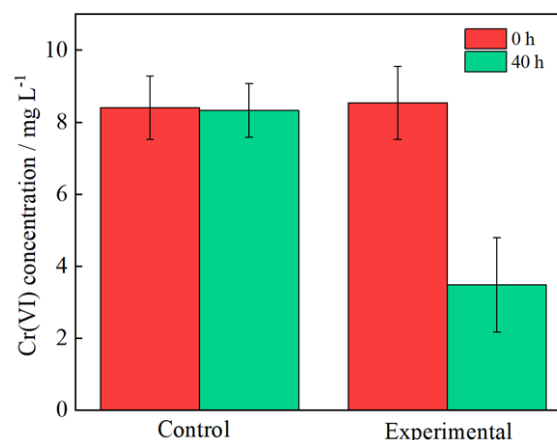


**Figure 1.** The Cr(VI) reduction in LB media containing Cr(VI) concentration of 8.5 mg/L without inoculated *C. freundii* A1B10 (Control) and with inoculated *C. freundii* A1B10 (Experimental).

### Whole-genome sequencing of *C. freundii* A1B10

The results showed that the estimated genome size was 4,927,083 base pairs (bp) with a gene number of 4,631 and a GC content of 52.11%. A total of 4,308 genes from *C. freundii* A1B10 strain were annotated with COG annotation, accounting for 93.03% of the total number of genes. The number of genes with unknown functions was the highest with a total of 323

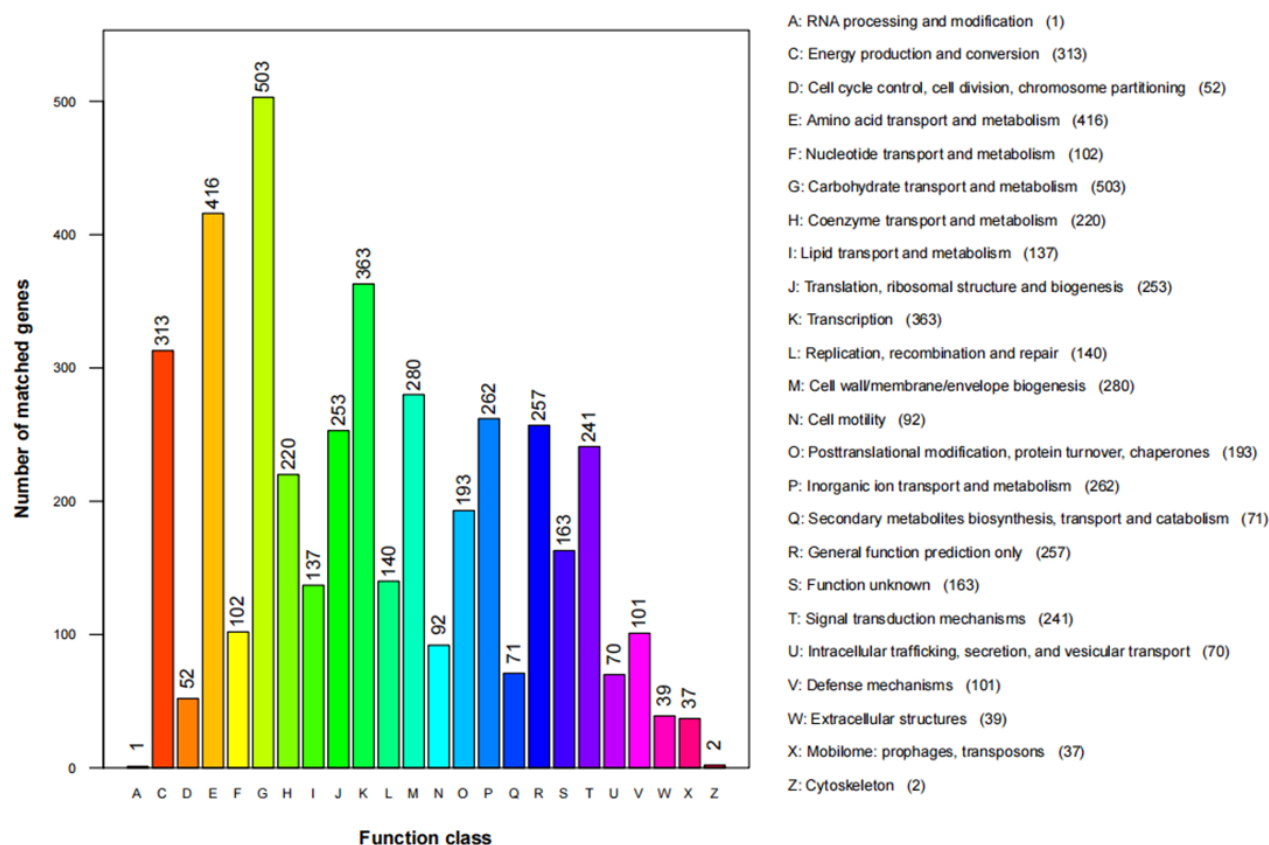


Figure 2. Gene function of *C. freundii* A1B10 based on COG database.

genes, accounting for 6.97% of the annotated genes. The functional classification of COGs related to heavy metal reduction was analyzed, and the results revealed that energy production and conversion, amino acid transport and metabolism, carbohydrate transport and metabolism, coenzyme transport and metabolism, translation, ribosomal structure and biogenesis, transcription, cell wall/membrane/envelope biogenesis, inorganic ion transport and metabolism, general function prediction only, signal transduction mechanisms accounted for 313, 416, 503, 220, 253, 363, 280, 262, 257, 241 genes, respectively, representing 7.27%, 9.66%, 11.68%, 5.11%, 5.88%, 8.43%, 6.50%, 6.08%, 5.97%, 5.59% of the total number of annotated genes (Figure 2). The whole-genome map of *C. freundii* A1B10 genes was then drawn (Figure 3). The whole-genome DNA sequence of *C. freundii* A1B10 was submitted to National Center for Biotechnology Information

(NCBI) (<https://www.ncbi.nlm.nih.gov/>) with the BioSample accession number of SAMN47739824.

### Cr(VI) resistance genes of *C. freundii* A1B10

Previous studies have identified multiple molecular determinants implicated in microbial Cr(VI) resistance mechanisms including sulfate transporters, phosphate transporters, molybdate uptake systems, chromate reductase, cytochrome c complexes, nitrite reductase, and proton-coupled electron transport systems [24-26]. Guided by this mechanistic framework, a comprehensive genomic survey was conducted to delineate the Cr(VI) resistance determinants in *C. freundii* A1B10. The results showed that the sulfate transport system proteins were encoded by genes *ettA*, *cysA*, *cysW*, *cysU*, and *cysP* in *C. freundii* A1B10. The phosphate transport system proteins were encoded by genes *pstS*, *pstC*, *pstA*, *pstB*, and *phoU* in *C. freundii* A1B10. Similarly, molybdate transport system components were

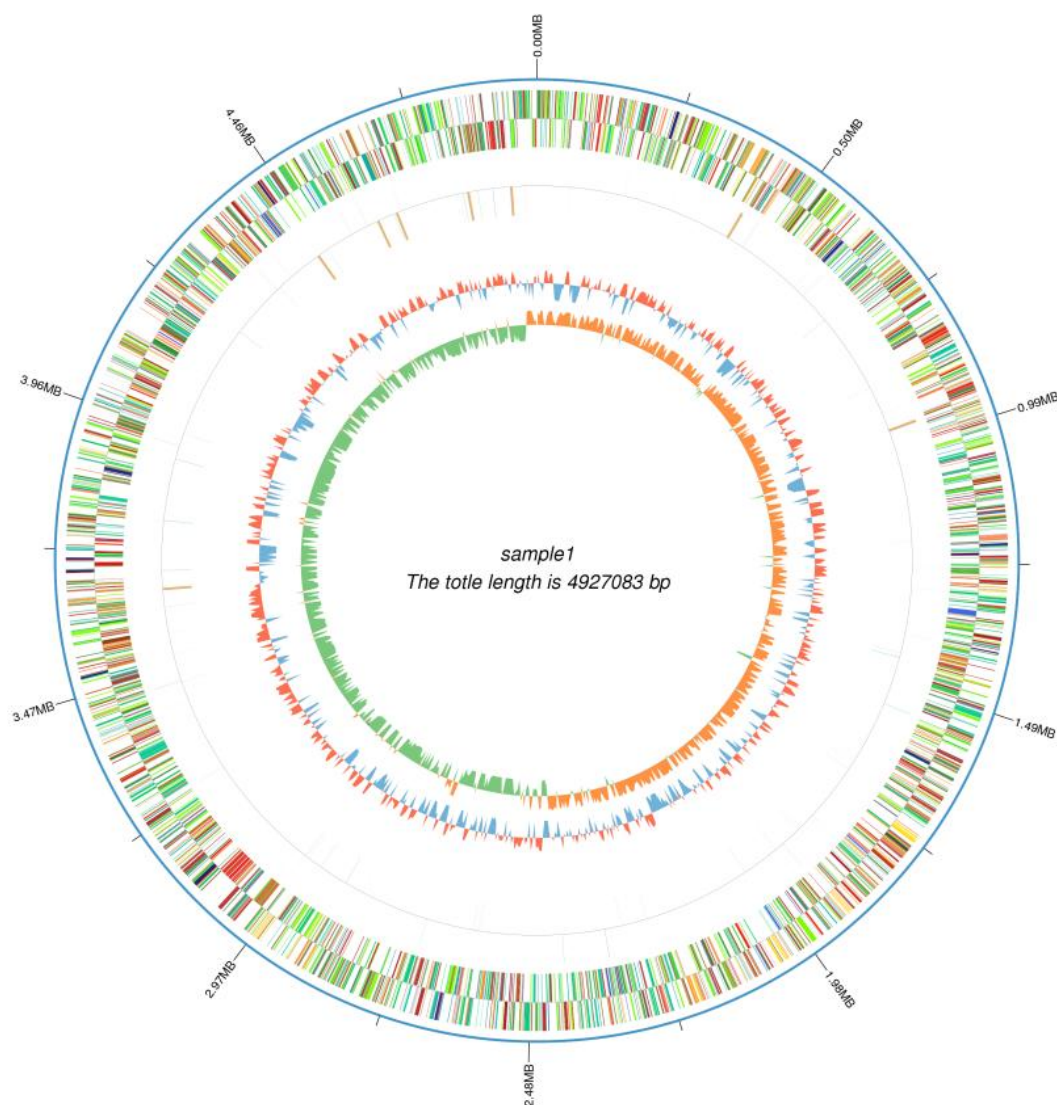


**Figure 3.** Whole genome map *C. freundii* A1B10. The visualization displayed genomic position coordinates in the outermost layer with successive inward layers representing functional gene annotations (COG), ncRNA distributions, and genomic GC content profiles from periphery to center.

encoded by the genes *modF*, *modC*, *modE*, *modB*, and *modA* in *C. freundii* A1B10. Chromate reductase production was directed by *chrR*, while nitrite reductase synthesis involved the *nirD*, *nirB*, and *nrfA* genes in *C. freundii* A1B10. Genes *ccmH*, *ccmF*, *ccmE*, *ccmG*, *nrfE*, *napC*, *napB*, *nrfB*, *torC*, *torA*, *torY*, *torZ*, *fbhH*, and *petA* in *C. freundii* A1B10 could encode cytochrome c. Genes *atpB*, *atpE*, *atpF*, *atpH*, *atpA*, *atpG*, *atpD*, and *atpC* in *C. freundii* A1B10 could encode proton transport proteins. The cytochrome oxidase systems in *C. freundii* A1B10 demonstrated distinct genetic organization with cytochrome bd oxidases being

encoded by the genes *appX*, *cydB*, *cydA*, and *cydX*, while cytochrome o oxidases production involving the genes of *cyoD*, *cyoB*, *cyoA*, and *cyoC* (Table 1).

## Discussion

In this study, *C. freundii* A1B10 was able to reduce Cr(VI), which was the same as that of *Citrobacter* sp. reported by Li *et al.* [22]. This might involve complex intracellular and extracellular reduction mechanisms [6, 14]. Therefore, the genes related

**Table 1.** Chromium resistance related genes.

| Gene name   | Gene production  | Gene function       |
|---|--|---------------------|
| <i>ettA</i>   | sulfate-transporting ATPase  | Sulfate transport   |
| <i>cysA</i>   | sulfate transport system ATP-binding protein                               |                     |
| <i>cysW, cysU</i>                                     | sulfate transport system permease protein                                  |                     |
| <i>cysP</i>   | sulfate transport system substrate-binding protein                         |                     |
| <i>pstS</i>   | phosphate transport system substrate-binding protein                       | Phosphate transport |
| <i>pstC, pstA</i>                                     | phosphate transport system permease protein                                |                     |
| <i>pstB</i>   | phosphate transport system ATP-binding protein                             |                     |
| <i>phoU</i>   | phosphate transport system protein   |                     |
| <i>modF, modC</i>                                     | molybdate transport system ATP-binding protein                             | Molybdate transport |
| <i>modE, modB</i>                                     | molybdate transport system regulatory protein                              |                     |
| <i>modA</i>   | molybdate transport system substrate-binding protein                       |                     |
| <i>chrR</i>   | chromate reductase, NAD(P)H dehydrogenase (quinone)                        | Chromate reductase  |
| <i>nirD</i>   | nitrite reductase (NADH) small subunit                                     | Nitrite reductase   |
| <i>nirB</i>   | nitrite reductase (NADH) large subunit                                     |                     |
| <i>nrfA</i>   | nitrite reductase (cytochrome c-552)                                       |                     |
| <i>ccmH, ccmF, ccmE, ccmG, nrfE, napC, napB, nrfB</i> | cytochrome c-type protein  | Cytochrome c        |
| <i>torC, torA, torY, torZ</i>                         | trimethylamine-N-oxide reductase (cytochrome c), cytochrome c-type subunit |                     |
| <i>fbhH</i>   | ubiquinol-cytochrome c reductase cytochrome b/c1 subunit                   |                     |
| <i>petA</i>   | ubiquinol-cytochrome c reductase iron-sulfur subunit                       |                     |
| <i>atpB atpE atpF, atpH, atpA, atpG, atpD, atpC</i>   | F-type H <sup>+</sup> -transporting ATPase subunit a                       | Proton transport    |
| <i>appX, cydB, cydA, cydX</i>                         | cytochrome bd-II ubiquinol oxidase subunit                                 | Electronic efflux   |
| <i>cyoD, cyoB, cyoA, cyoC</i>                         | cytochrome o ubiquinol oxidase subunit IV                                  |                     |

to chromium resistance in *C. freundii* A1B10 were analyzed by whole genome sequencing to elucidate this mechanism.

Transmembrane transport is a critical pathway for Cr(VI) entry into biological cells. Previous studies have demonstrated that Cr(VI) enters cells in the form of chromate ions (CrO<sub>4</sub><sup>2-</sup>) through inorganic anion transport pathways, leading to DNA damage and cellular metabolic dysfunction *via* complex competitive inhibition effects [27]. The mechanism by which CrO<sub>4</sub><sup>2-</sup> enters cells *via* sulfate transport systems is well established [28]. Due to the structural similarity between CrO<sub>4</sub><sup>2-</sup> and sulfate ions (SO<sub>4</sub><sup>2-</sup>), CrO<sub>4</sub><sup>2-</sup> competes with SO<sub>4</sub><sup>2-</sup> for transport carriers to gain intracellular access [29]. Notably, CrO<sub>4</sub><sup>2-</sup> transmembrane transport exhibits multi-channel characteristics. Plant studies have confirmed that CrO<sub>4</sub><sup>2-</sup> can enter cells through phosphate transporters [30]. Compared to H<sub>2</sub>PO<sub>4</sub><sup>-</sup>, CrO<sub>4</sub><sup>2-</sup>

shows higher chemical structural compatibility with phosphate transporters and forms stable binding interactions, facilitating its entry *via* these transporters [31]. Additionally, CrO<sub>4</sub><sup>2-</sup> and molybdate ions (MoO<sub>4</sub><sup>2-</sup>) share structural similarities, both adopting tetrahedral configurations. The Mo-O bond length (1.79 Å) is comparable to the Cr-O bond length (1.686 Å), suggesting potential involvement of molybdate transport systems in cellular Cr(VI) uptake [32, 33]. Studies indicated that the expression levels of microbial molybdate transporter genes *modA*, *modB*, *modC* were significantly upregulated in the presence of Cr(VI) [34], which implied that CrO<sub>4</sub><sup>2-</sup> might enter cells *via* molybdate transporters, while microorganisms might upregulate molybdate transporter expression to compensate for the demand of MoO<sub>4</sub><sup>2-</sup> transport channels to maintain molybdenum homeostasis. Therefore, in *C. freundii* A1B10, the genes encoding sulfate transporters (*ettA*, *cysA*, *cysW*,



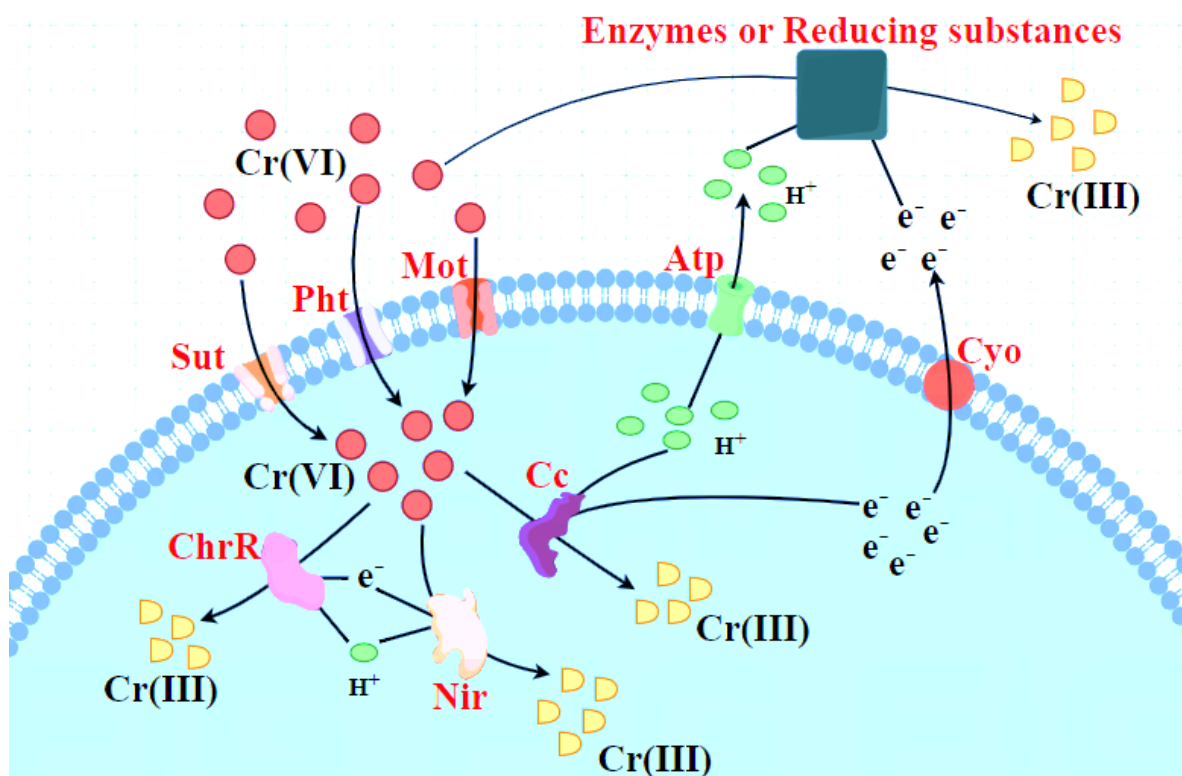


**Figure 4.** Schematic model of *C. freundii* A1B10 to reduce Cr(VI). Sut: sulfate transport system protein. Pht: phosphate transport system protein. Mot: molybdate transport system protein. Atp: proton transport protein. Cyo: cytochrome oxidase. ChrR: chromate reductase. Nir: nitrite reductase. Cc: cytochrome c.

*cysU*, *cysP*), phosphate transporters (*pstS*, *pstC*, *pstA*, *pstB*, *phoU*), and molybdate transporters (*modF*, *modC*, *modE*, *modB*, *modA*) are associated with cellular Cr(VI) uptake.

Microbial reduction of Cr(VI) can be categorized into extracellular and intracellular reduction. Numerous studies have demonstrated that most microorganisms can secrete chromate-reducing enzymes to reduce highly toxic Cr(VI) to less toxic Cr(III) [35, 36]. Regardless of whether intracellular reduction or extracellular reduction occurred, the process of Cr(VI) reduction by microorganism requires the participation of  $H^+$  and electrons [37]. The genes *atpB*, *atpE*, *atpF*, *atpH*, *atpA*, *atpG*, *atpD*, *atpC* can encode proton transport proteins in *C. freundii* A1B10. The genes *appX*, *cydB*, *cydA*, *cydX*, *cyoD*, *cyoB*, *cyoA*, *cyoC* can encode cytochrome oxidase in *C. freundii* A1B10. These genes may play an important role in maintaining intracellular and extracellular

proton and electron balance and promoting extracellular hexavalent chromium reduction. However, there are few reports on extracellular chromate reductase. It has been found that cytochrome c, quinone oxidoreductase ChrR and nitrite reductase have chromate reducing activity in the cell, which can reduce Cr(VI) to Cr(III). Therefore, the ChrR encode gene *chrR*, the cytochrome c encode genes *ccmH*, *ccmF*, *ccmE*, *ccmG*, *nrfE*, *napC*, *napB*, *nrfB*, *torC*, *torA*, *torY*, *torZ*, *fbhH*, *petA*, and the nitrite reductase encode genes *nirD*, *nirB*, *nrfA* in *C. freundii* A1B10 may play the role of reducing Cr(VI) to Cr(III) in the cell to reduce the toxicity of Cr(VI) to cells. Based on the above analysis, the mechanism diagram of reduction of Cr(VI) by *C. freundii* A1B10 was speculated (Figure 4). The sulfate transporters (Sut), phosphate transporters (Pht), and molybdate transporters (Mot) are associated with cellular Cr(VI) uptake. The proton transport proteins (Atp) and cytochrome oxidase (Cyo) play

an important role in maintaining intracellular and extracellular proton and electron balance and promoting extracellular hexavalent chromium reduction. The ChrR, cytochrome c (Cc), and nitrite reductase (Nir) play the role of reducing Cr(VI) to Cr(III) in the cell.

### Acknowledgements

This research was supported by the Key Science & Technology Specific Projects of Henan Province (Grant No. 191110110600), Natural Science Foundation of Henan Province (Grant No. 242300421627 and 252300420703), Science and Technology Innovation Youth Project of Zhumadian City (Grant No. QNZX202318), Major Scientific and Technological Innovation Project of Zhumadian City (Grant No. ZMDSZDX2023007).

### References

- Murthy MK, Khandayataray P, Padhiary S, Samal D. 2023. A review on chromium health hazards and molecular mechanism of chromium bioremediation. *Rev Environ Health*. 38(3):461-478.
- Román Abarca ME, Kar T, Casales-Díaz M, Ramos-Hernández JJ, Godavarthi S, Reddy Bogireddy NK, *et al.* 2025. Effective photocatalytic chromium (VI) detoxification with metal-free heterojunction based on g-C(3)N(5) and ZIF-8 carbon under visible light. *Environ Res*. 275:121424.
- Hua T, Li Y, Hu Y, Yin R, Zhang Y, Hou B, *et al.* 2025. Back to chromite as a mineralogical strategy for long-term chromium pollution control. *Nat Commun*. 16(1):1975.
- Balasaraswathi K, Jayaveni S, Sridevi J, Sujatha D, Phebe Aaron K, Rose C. 2017. Cr-induced cellular injury and necrosis in *Glycine max* L.: Biochemical mechanism of oxidative damage in chloroplast. *Plant Physiol Biochem*. 118:653-666.
- Soliman ERS, Moustafa K, Khamis M, Shedeed ZA. 2025. Chromium "(VI)" phytoremediation using *Azolla pinnata*: effects on *Vicia faba* growth, physiology, cytogenetics, and gene expression profiling. *BMC Plant Biol*. 25(1):160.
- Cao L, Lu M, Zhao M, Zhang Y, Nong Y, Hu M, *et al.* 2023. Physiological and transcriptional studies reveal Cr(VI) reduction mechanisms in the exoelectrogen *Cellulomonas fimi* Clb-11. *Front Microbiol*. 14:1161303.
- Xu H, Ren L, Jie W, Zhang H, Zhao Y. 2024. Transformation of iron-minerals from natural aquifer media by sulfate-reducing bacteria: Behavior, mechanism, and Cr(VI) removal. *Sci Total Environ*. 955:177021.
- Zhao S, Chen Z, Wang B, Shen J, Zhang J, Li D. 2018. Cr(VI) removal using different reducing agents combined with fly ash leachate: A comparative study of their efficiency and potential mechanisms. *Chemosphere*. 213:172-181.
- Peng M, Gan M, Zhao X, Zhu J, Zhang K. 2025. Self-modified iron-based materials for efficient chromium (VI) removal: Efficacy and mechanism. *Environ Res*. 272:121193.
- Kong F, Wang W, Wang X, Yang H, Tang J, Li Y, *et al.* 2025. Performance and mechanism of nano Fe-Al bimetallic oxide enhanced constructed wetlands for the treatment of Cr(VI)-contaminated wastewater. *Environ Res*. 271:121154.
- Zheng X, Tong J, Zhou S, Liu Y, Liu G, Zou D. 2024. Remediation of hexavalent chromium contaminated soils by stimulating indigenous microorganisms: Optimization, community succession and applicability. *J Environ Manage*. 372:123222.
- Shruthi S, Hemavathy RV. 2024. Myco-remediation of chromium heavy metal from industrial wastewater: A review. *Toxicol Rep*. 13:101740.
- Priyadarshane M, Das S. 2024. Multifaceted response surface methodology unravels competitive heavy metal adsorption affinity of immobilized biosorbent formulated from bacterial extracellular polymer of *Pseudomonas aeruginosa* OMCS-1. *Chemosphere*. 368:143681.
- Sun H, Li Y, Gao S, Shi G, Cao L, Li X, *et al.* 2025. Identification of key chromium resistance genes in *Cellulomonas* using transcriptomics. *Ecotoxicol Environ Saf*. 291:117843.
- Jiang C, Hu L, He N, Liu Y, Zhao H, Jiang Z. 2024. Different calcium sources affect the products and sites of mineralized Cr(VI) by microbially induced carbonate precipitation. *Chemosphere*. 363:142977.
- Gu Y, Xu W, Liu Y, Zeng G, Huang J, Tan X, *et al.* 2015. Mechanism of Cr(VI) reduction by *Aspergillus niger*: Enzymatic characteristic, oxidative stress response, and reduction product. *Environ Sci Pollut Res Int*. 22(8):6271-6279.
- Liu T, Luo X, Wu Y, Reinfelder JR, Yuan X, Li X, *et al.* 2020. Extracellular electron shuttling mediated by soluble c-Type cytochromes produced by *Shewanella oneidensis* MR-1. *Environ Sci Technol*. 54(17):10577-10587.
- Sundarraj S, Sudarmani DNP, Samuel P, Sevarkodiyone SP. 2022. Bioremediation of hexavalent chromium by transformation of *Escherichia coli* DH5α with chromate reductase (ChrR) genes of *Pseudomonas putida* isolated from tannery effluent. *J Appl Microbiol*. 134(1):lxac019.
- Francisco R, de Abreu P, Plantz BA, Schlegel VL, Carvalho RA, Morais PV. 2011. Metal-induced phosphate extracellular nanoparticulate formation in *Ochrobactrum tritici* 5bvl1. *J Hazard Mater*. 198:31-39.
- Li ZT, Song X, Yuan S, Zhao HP. 2024. Unveiling the inhibitory mechanisms of chromium exposure on microbial reductive dechlorination: Kinetics and microbial responses. *Water Res*. 253:121328.
- Wang Q, Zhang C, Song J, Bamanu B, Zhao Y. 2024. Inhibitory mechanism of Cr(VI) on sulfur-based denitrification: Bio-toxicity, bio-electron characteristics, and microbial evolution. *J Hazard Mater*. 472:134447.
- Li X, Fan M, Zhang Y, Liu L, Yi F, Chang J, *et al.* 2021. Remediation of chromium- and fluoride-contaminated groundwater by immobilized *Citrobacter* sp. on a nano-ZrO<sub>2</sub> hybrid material. *PLoS one*. 16(6):e0253496.



23. Cao L, Ma Y, Deng D, Jiang H, Wang J, Liu Y. 2020. Electricity production of microbial fuel cells by degrading cellulose coupling with Cr(VI) removal. *J Hazard Mater.* 391:122184.
24. Lin WH, Chen CC, Ou JH, Sheu YT, Hou D, Kao CM. 2022. Bioremediation of hexavalent-chromium contaminated groundwater: Microcosm, column, and microbial diversity studies. *Chemosphere.* 295:133877.
25. Thatoi H, Das S, Mishra J, Rath BP, Das N. 2014. Bacterial chromate reductase, a potential enzyme for bioremediation of hexavalent chromium: A review. *J Environ Manage.* 146:383-399.
26. Shi L, Zhao X, Zhong K, Jia Q, Shen Z, Zou J, *et al.* 2022. Physiological mechanism of the response to Cr(VI) in the aerobic denitrifying ectomycorrhizal fungus *Pisolithus* sp.1. *J Hazard Mater.* 429:128318.
27. Tang Y, Zhang B, Li Z, Deng P, Deng X, Long H, *et al.* 2023. Overexpression of the sulfate transporter-encoding SULTR2 increases chromium accumulation in *Chlamydomonas reinhardtii*. *Biotechnol Bioeng.* 120(5):1334-1345.
28. Lara P, Vega-Alvarado L, Sahonero-Canavesi DX, Koenen M, Villanueva L, Riveros-Mckay F, *et al.* 2021. Transcriptome analysis reveals Cr(VI) adaptation mechanisms in *Klebsiella* sp. strain AqSCr. *Front Microbiol.* 12:656589.
29. Su YQ, Min SN, Jian XY, Guo YC, He SH, Huang CY, *et al.* 2023. Bioreduction mechanisms of high-concentration hexavalent chromium using sulfur salts by photosynthetic bacteria. *Chemosphere.* 311(Pt 1):136861.
30. Li J, Xie W, Qi H, Sun S, Deng T, Tang Y, *et al.* 2024. Hexavalent chromium uptake in rice (*Oryza sativa* L.) mediated by sulfate and phosphate transporters OsSultr1;2 and OsPht1;1. *J Hazard Mater.* 478:135559.
31. Bouhadi M, Daoui O, El Hajjouji H, Elkhatabi S, Chtita S, El Kouali M, *et al.* 2023. Study of the competition between Pi and Cr (VI) for the use of Pi-transporter at *Vicia faba* L. using molecular modeling. *Plant Physiol Biochem.* 196:695-702.
32. Busayaporn W, Songsrirote K, Phlialamkheak T, Chumram J, Praingam N, Prayongpan P. 2023. Synthesis and application of fluorescent N-doped carbon dots/hydrogel composite for Cr(VI) adsorption: Uncovering the ion species transformation and fluorescent quenching mechanism. *Environ Geochem Health.* 45(7):5293-5309.
33. Kaur P, Kumar R, Davessar S, Khanna A. 2020. Structural and optical characterization of Er-doped CaMoO(4) down-converting phosphors. *Acta Crystallogr B Struct Sci Cryst Eng Mater.* 76(Pt 5):926-938.
34. Shi Y, Wang Z, Li H, Yan Z, Meng Z, Liu C, *et al.* 2023. Resistance mechanisms and remediation potential of hexavalent chromium in *Pseudomonas* sp. strain AN-B15. *Ecotoxicol Environ Saf.* 250:114498.
35. Zhang Y, Sang P, Wang K, Gao J, Liu Q, Wang J, *et al.* 2024. Enhanced chromium and nitrogen removal by constructing a biofilm reaction system based on denitrifying bacteria preferential colonization theory. *Ecotoxicol Environ Saf.* 273:116156.
36. Jia B, Wan J, Liu H, Yan B, Zhang L, Su X. 2023. DIET-like and MIET-like mutualism of *S. oneidensis* MR-1 and metal-reducing function microflora boosts Cr(VI) reduction. *J Hazard Mater.* 465:133401.
37. Liao Q, Tang J, Wang H, Yang W, He L, Wang Y, *et al.* 2020. Dynamic proteome responses to sequential reduction of Cr(VI) and adsorption of Pb(II) by *Pannonibacter phragmitetus* BB. *J Hazard Mater.* 386:121988.